*The American Journal of Pathology, Vol. 173, No. 6, December 2008*

*DOI: 10.2353/ajpath.2008.080407*

*Immunopathology and Infectious Diseases*

# Genetic Inversion in Mast Cell-Deficient $W^{sh}$ Mice Interrupts *Corin* and Manifests as Hematopoietic and Cardiac Aberrancy

Peter A. Nigrovic,*† Daniel H.D. Gray,‡ Tatiana Jones,* Jenny Hallgren,* Frank C. Kuo,§ Blair Chaletzky,* Michael Gurish,* Diane Mathis,*‡ Christophe Benoist,*‡ and David M. Lee*

*From the Division of Rheumatology, Immunology and Allergy,* Brigham and Women's Hospital, Boston; the Division of Immunology,† Children's Hospital Boston, Boston; the Section on Immunology and Immunogenetics,‡ Joslin Diabetes Center, Boston; and the Department of Pathology,§ Brigham and Women's Hospital, Boston, Massachusetts*

**Mast cells participate in pathophysiological processes that range from antimicrobial defense to anaphylaxis and inflammatory arthritis. Much of the groundwork for the understanding of mast cells was established in mice that lacked mast cells through defects in either stem cell factor or its receptor, Kit. Among available strains, C57BL/6-*Kit*$^{W\text{-}sh}$ ($W^{sh}$) mice are experimentally advantageous because of their background strain and fertility. However, the genetic inversion responsible for the $W^{sh}$ phenotype remains poorly defined, and its effects beyond the mast cell have been incompletely characterized. We report that $W^{sh}$ animals exhibit splenomegaly with expanded myeloid and megakaryocyte populations. Hematopoietic abnormalities extend to the bone marrow and are reflected by neutrophilia and thrombocytosis. In contrast, mast cell-deficient WBB6F1-*Kit*$^{W}$/*Kit*$^{W\text{-}v}$ ($W/W^{v}$) mice display mild neutropenia, but no changes in circulating platelet numbers. To help define the basis for the $W^{sh}$ phenotype, a "DNA walking" strategy was used to identify the precise location of the 3′ breakpoint, which was found to reside 67.5 kb upstream of *Kit*. The 5′ breakpoint disrupts *corin*, a cardiac protease responsible for the activation of atrial natriuretic peptide. Consistent with this result, transcription of full-length *corin* is ablated and $W^{sh}$ mice develop symptoms of cardiomegaly. Studies performed using mast cell-deficient strains must consider the capacity of associated abnormalities to either expose or compensate for the missing mast cell lineage.** ***(Am J Pathol 2008, 173:1693–1701; DOI: 10.2353/ajpath.2008.080407)***

Mast cells arise as precursors in the bone marrow and mature within the tissues, where they participate in both allergic and nonallergic immune processes. Phylogenetic studies confirm that this lineage predates the development of humoral immunity, implying that participation in IgE-mediated responses is a rather late specialization.[1] Indeed, mast cells have now been implicated in a broad range of pathophysiologic processes, where they most typically initiate or amplify immune responses via rapid release of preformed and newly synthesized mediators. One important role in this regard is the mobilization of defenses against bacteria and parasites.[2–6] Rapid mediator release also has pathogenic consequences, such as anaphylaxis or the initiation phase of inflammatory arthritis.[7,8] Beyond this "sentinel" role, mast cells participate in the neutralization of venoms and inflammatory mediators as well as other biological processes (reviewed in[9]).

These conclusions have been reached largely through experiments in mice with spontaneous genetic mutations that perturb mast cell differentiation. Mast cells at all stages of maturation express the receptor tyrosine kinase Kit (CD117) and require the Kit ligand, stem cell factor (SCF), for their survival. Most laboratory strains deficient in mast cells arise from mutations affecting the Kit/SCF axis. For example, the WCB6F1/J-*Kitl*$^{Sl}$/*Kitl*$^{Sl\text{-}d}$ mouse lacks SCF on the surface of fibroblasts and other cells.[10] The $W/W^{v}$ mouse bears a compound mutation (one allele

Supported by K08-AR051321 (P.A.N.); Australian National Health and Medical Research Council CJ Martin Overseas Biomedical Fellowship (D.H.D.G.); Juvenile Diabetes Research Foundation, P01 AI065858-02, Young Chair funds (D.M., C.B.); and R01-AI059745, P01 AI065858-02, and the Cogan Family Foundation (D.M.L.).

Accepted for publication September 9, 2008.

Address reprint requests to David M. Lee, M.D., Ph.D., Division of Rheumatology, Immunology and Allergy, Brigham and Women's Hospital, One Jimmy Fund Way, Smith 552B, Boston MA 02115. E-mail: dlee@rics.bwh.harvard.edu.

null, the other impaired) at the *Kit* locus W (white spotting), while the $W^{sh}$ mouse carries an incompletely characterized inversion upstream of *Kit* that affects a key regulatory element.[11–16] Mice with mutations affecting *Kit* (rather than SCF) are particularly useful because they can be engrafted with cultured mast cells.[17,18] An abnormal phenotype that can be corrected with such engraftment may presumptively be attributed to mast cell deficiency.

Such complementation studies are important because mutations affecting *Kit* have effects beyond the mast cell lineage. For example, the $W/W^{v}$ mouse is white, anemic, partially deaf, prone to dermatitis and gastritis, and lacks intestinal interstitial cells of Cajal, as well as intraepithelial $\gamma\delta$ T lymphocytes (reviewed in[18]). Bone marrow and circulating neutropenia have also been described.[19,20] Further, $W/W^{v}$ mice are sterile, so colony maintenance and breeding are cumbersome, and control mice are WBB6 heterozygotes. $W^{sh}$ mice are also white (the heterozygote exhibiting a white abdominal sash, providing the strain name, the homozygote having residual ear pigment), but they are not anemic and are fully fertile. Other hematological lineages have been considered normal based on the comparison of limited numbers of $W^{sh}$ and C57BL/6 animals.[18,20] The breeding advantage and C57BL/6 background strain (from backcrossing, after the mutation arose spontaneously during a cross between C3H/HeH and 101/H)[21] have made $W^{sh}$ mice recent favorites for work in the mast cell field.

In initial analyses of $W^{sh}$ mice, it was noted that some animals had strikingly enlarged and histologically abnormal spleens. Given the increasing importance of the $W^{sh}$ strain in mast cell research, we wished to better understand "off-target" hematological effects of the large gene inversion in these animals, since associated abnormalities could alter experimental interpretation. The results presented herein provide an expanded phenotypic and genotypic characterization of this important experimental strain, and suggest that experimental results obtained in both $W^{sh}$ and $W/W^{v}$ must be interpreted in light of the potential role of accompanying abnormalities on the phenotype of interest.

## Materials and Methods

### Mice

WBB6 F1-$Kit^{W}/Kit^{W\text{-}v}$ ($W/W^{v}$), WBB6 littermate controls and C57BL/6J (B6) mice were purchased from The Jackson Laboratory (Bar Harbor, ME). C57BL/6-$Kit^{W\text{-}sh/W\text{-}sh}$ mice[22] were maintained at The Jackson Laboratory. Animals were housed for at least 2 weeks in the specific-pathogen-free animal facility of the Dana-Farber Cancer Institute before sacrifice for phenotyping experiments. All procedures were approved by the animal care and use committees of the Dana-Farber Cancer Institute or Harvard Medical School.

### Hematological and Cardiac Phenotyping

Age-matched male mice ($W/W^{v}$ and WBB6: 12 to 20 weeks, $W^{sh}$ and B6: 10 to 15 weeks, except as noted) were anesthetized with isofluorane for bleeding by cardiac puncture. Whole blood was collected in the presence of EDTA to prevent clotting. A complete blood count and automated leukocyte differential was obtained using an Advia 120 Hematology System (Siemens, Tarrytown, NY) and appropriate species-specific standards and software. The accuracy of the automated neutrophil assessment was confirmed by parallel flow cytometric examination of selected blood samples stained for CD45 and Gr-1 (data not shown). Spleens were removed, cleaned of attached tissues, and weighed. Remaining splenic tissue was disaggregated and filtered through 100 $\mu$m mesh for cytofluorometric analysis. Hearts were removed, cleaned of excess soft tissue, and compressed to expel luminal blood before weighing. Femoral bone marrow was obtained by flush and passed through 100-$\mu$m mesh to separate adherent cells and exclude bone fragments. Tissue taken for histology was fixed in 4% paraformaldehyde in PBS.

### Cytofluorimetry

Samples were washed in PBS with 10% fetal bovine serum and stained with appropriate antibodies and isotype controls. Cytofluorometric analysis was performed using a FACSDiva cytometer (Becton-Dickinson, Franklin Lakes, NJ). All samples were co-stained with 7-aminoactinomycin D (7-AAD) and anti-CD45.2 (BD Biosciences, Franklin Lakes, NJ), and gated to include only viable (7-AAD negative) CD45+ cells. Other antibodies used were as follows: CD3-flurorescein isothiocyanate, CD41-phycoerythrin (BD Biosciences), CD11b-flurorescein isothiocyanate, CD117-Alexa647, F4/80-phycoerythrin, Gr-1-flurorescein isothiocyanate, Gr-1-Alexa647 (Invitrogen, Carlsbad, CA), CD11c-allophycocyanin, CD19-phycoerythrin (eBioscience, San Diego, CA).

### Mast Cell Progenitor Assay

Mast cell progenitors were enumerated by limiting dilution analysis, as described.[23] Briefly, splenic mononuclear cells were isolated from disaggregated splenocytes via Percoll gradient, enumerated, and cultured by limiting dilution in the presence of irradiated syngenic feeder splenocytes and baculovirus-generated SCF and interleukin-3 (both at 20 ng/ml final). Culture media was RPMI 1640 supplemented with 10% fetal calf serum, glutamine (2 mmol/L), penicillin (100 U/ml), streptomycin (100 $\mu$g/ml), gentamicin (50 $\mu$g/ml), pyruvate (1 mmol/L), nonessential amino acids, Hepes (10 mmol/L), and 2-mercaptoethanol (50 $\mu$mol/L). The mast cell colonies with their distinct morphology were counted at 10 to 14 days. While committed mast cell progenitors have typically been enumerated in peripheral tissues with this technique,[24] myeloid progenitors upstream of committed mast cell progenitors that are SCF- and/or interleukin-3-responsive

would also be expected to form colonies in this assay.[25] Thus this assay enumerates the cells capable of giving rise to committed mast cells within this tissue.

### *Microscopy*

Histological sections were stained with H&E, and examined at ×100 and ×400 using a Leica DM LB2 microscope and Leica digital camera.

### *Inversion Breakpoint Identification*

The 5′-breakpoint of the W$^{sh}$ inversion mutation was located by PCR with primers that yield a 600-bp product from wild-type (C57BL/6J), but not W$^{sh}$ template (WT-for, 5′-TTTG-CACGTGCTA GTTACAC-3′; WT-rev, 5′-TTAAGATGGCAC-CCTGCTG-3′). A series of three nested PCR primers was designed for sequencing 5′ to the distal breakpoint (TSP1, 5′-C CTCAGCCTGTCACACTTATG-3′; TSP2, 5′-GACAAC-GAAATGATACAGAG GATTC-3′; TSP3, 5′-GAGGATTCAT-AGTTGTTCAATGTCC-3′), and were used with the DNA Walking Speedup Kit (Seegene, Rockville, MD) to amplify a single 500-bp product from W$^{sh}$, but not WT template. Confirmatory PCR primers flanking the predicted breakpoint were designed (W$^{sh}$-for, 5′-AGGCTTGCAGCGCATTAT-3′; W$^{sh}$-rev, 5′-GAGGATTCATAGTTGTTCAATGTCC-3′). The "WT" and "W$^{sh}$" primers can be used for genotyping purposes with the PCR program: 94°C for 5 minutes, followed by 35 cycles of 94°C for 20 seconds; 57°C for 30 seconds; 72°C for 1 minute, followed by 72°C for 10 minutes. Regions of *corin* intron 5 and exon 6 were amplified using the following primers: Int 5A-for, 5′-GGGGGATTGTTTCCAATTCT-3′; Int 5A-rev, 5′-TGGA CCTAGAGGGCATCATC-3′, Int 5B-for, 5′-TCAGCCATTCGGTATTCCTC-3′; Int 5B-rev, 5′-AAAAG-GCCACCAACAGATTG-3′; Exo 6-for, 5′-GGGGTTCT GGAAGGAAATCT-3′; Exo 6-rev, 5′-TCGCTCCAGTCAT CACAGTC-3′.

### *Quantitative PCR of* Corin *Transcription*

Total RNA was prepared from atria dissected from wild-type or W$^{sh}$ mice and cDNA synthesized using random primers. PCR was performed with SYBR Green Mastermix (Applied Biosystems, UK) using primers designed to *corin* exons 3 to 4 (forward-5′-TCCT TCTCCAGAGGACCAGA-3′; reverse-5′-AGGGCAGAATTTGACACTGG-3′), 5 to 6 (forward-5′-GCAGGAACATGGAAAGCAAT-3′; reverse-5′-TGGTACA-CAGGAA GCTCTCG-3′), or 10 to 11 (forward-5′-GACAGCAGCCTGAGTAACTGC-3′; reverse-5′-TGTAGGG CAAATTCATGCAG-3′) on a Mx3000p PCR machine (Stratagene, La Jolla, CA). Data were analyzed using the $2^{-\Delta\Delta Ct}$ method normalized to a single wild-type data set.[26]

### *Statistical Analysis*

Experimental strains were compared with background-control animals using the Student's *t*-test without correction for multiple comparisons. Data are expressed as mean ± SEM. *P* values ≤0.05 were considered significant.

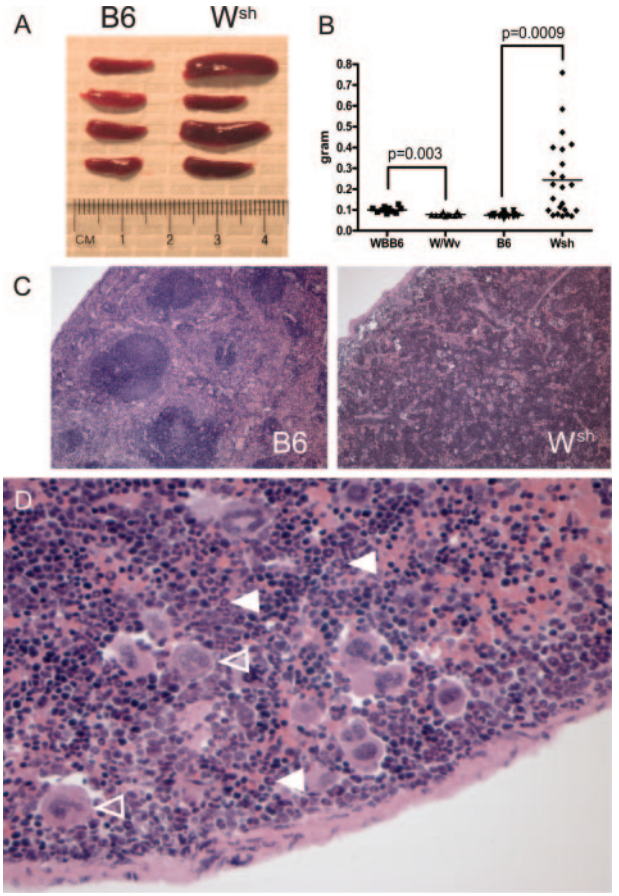


**Figure 1.** W$^{sh}$ animals exhibit gross and microscopic splenic abnormalities. **A:** Representative spleens from 12 week male B6 and matching W$^{sh}$ mice showing variable enlargement of W$^{sh}$ spleens even among littermates. **B:** Quantitation of spleen mass from age-matched mast cell-deficient mice and controls, $n$ = 10 (WBB6 and W/W$^{v}$), $n$ = 22 (B6), $n$ = 23 (W$^{sh}$). **C:** H&E staining of B6 and W$^{sh}$ spleens from 12-week-old mice (magnification = original ×100). Note the clear separation of white pulp and red pulp in B6 that is lost in W$^{sh}$, along with the appearance of large multinucleated cells. This phenotype is observed typically in larger W$^{sh}$ spleens, while others may show relatively normal histology. **D:** High power image of W$^{sh}$ spleen (magnification = original ×400) demonstrating large multinucleated megakaryocytes (**open arrowheads**) and an abundance of neutrophil-lineage forms (**solid arrowheads**).

## *Results*

### *Expanded Myeloid and Megakaryocyte Populations in W$^{sh}$ Spleen*

Initial work with the W$^{sh}$ mice was notable for several splenic abnormalities. Even among littermates, a striking divergence of spleen size was readily observed (Figure 1A–B). These changes were not explained by body mass, which was equivalent between W$^{sh}$ and B6 animals (body weight mean of male 12-week old mice $n$ = 15 to 18/group: W$^{sh}$ 25.5 ± 0.5g, B6 26.1 ± 0.4g, $P$ = 0.32). Histologically, splenic architecture ranged from normal to strikingly abnormal, with disrupted white pulp and abundant large multinucleated cells (Figure 1C). At higher power, these large cells were seen to be normal-appearing megakaryocytes, while abundant neutrophils were also evident (Figure 1D). Erythroid precursors were increased as well, indicating exaggerated trilineage he-

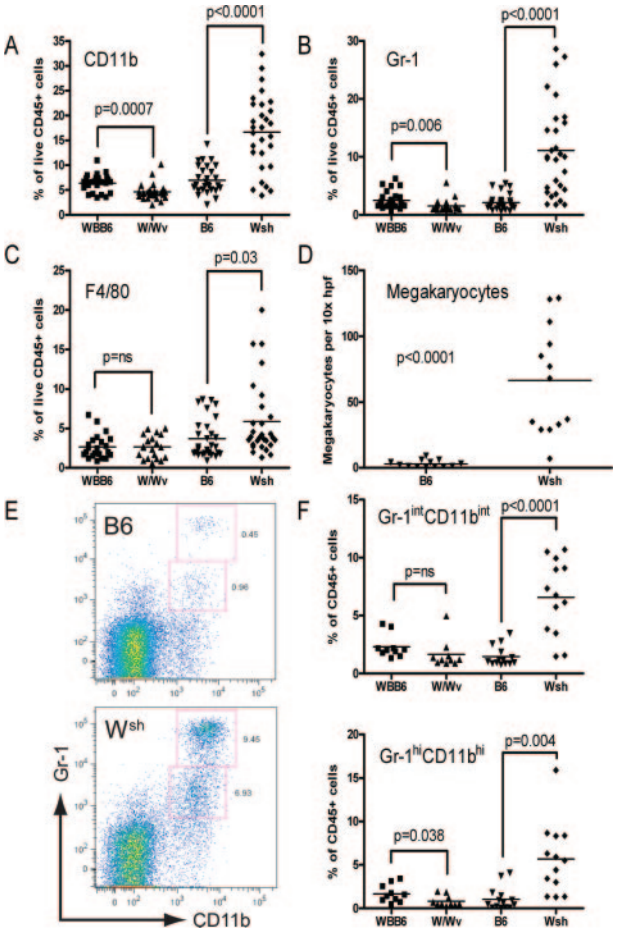


**Figure 2.** W/W$^v$ and W$^{sh}$ mice display contrasting myeloid aberrancy in spleen. Spleens from mast-cell deficient animals and age-matched controls were disaggregated and analyzed by cytofluorimetry and histomorphometry. Cytofluorimetric data reported are the percentage of viable, CD45+ cells in individual mice ($n$ = 10 to 26 W/W$^v$ and WBB6 mice and $n$ = 13 to 29 W$^{sh}$ and B6 mice pooled from 2 to 7 independent experiments). **A:** CD11b (component of Mac-1). **B:** Gr-1. **C:** F4/80. **D:** Megakaryocyte quantitation by histomorphometry (B6 3.0 ± 0.7 vs. W$^{sh}$ 66.3 ± 11.4 cells/10x hpf, $n$ = 13 male mice aged 10 to 14 weeks/group pooled from three experiments). **E:** Representative dot plots of viable CD45+ splenocytes showing two Gr-1+CD11b+ populations defined by expression level of these markers. **F:** Quantitation of Gr-1/CD11b-expressing populations.

matopoiesis. In contrast, W/W$^v$ spleens were slightly smaller than WBB6 controls and appeared histologically normal (Figure 1B and data not shown).

To evaluate these abnormalities, splenocyte populations were quantified by cytofluorimetry and histomorphometry. Consistent with an expansion of the myeloid compartment in many of the W$^{sh}$ mice, the proportion of cells expressing CD11b was elevated 2- to 3-fold, accompanied by a fivefold increase in cells expressing the myeloid marker Gr-1 and an almost twofold increase in cells expressing F4/80 (Figure 2, A–C). Reciprocal decreases were found in the proportion of splenic B and T cells (data not shown). Cells expressing the dendritic cell marker CD11c were present in normal proportions (data not shown). Histomorphometric enumeration of megakaryocytes demonstrated a greater than 20-fold increase in the number of cells visible in a splenic cross section, corresponding to a more than hundred-fold expansion extrapolated across three dimensions (Figure 2D). Since expression of CD11b together with Gr-1 is thought to mark a regulatory myeloid phenotype, coexpression of these antigens was examined.[27] Both Gr-1$^{hi}$CD11b$^{hi}$ and Gr-1$^{int}$CD11b$^{int}$ populations were expanded in W$^{sh}$ animals (Figure 2, E–F). Unlike W$^{sh}$ animals, W/W$^v$ mice showed a reduction in splenic CD11b+ cells, Gr-1+ cells, and Gr-1$^{hi}$ CD11b$^{hi}$ splenocytes compared with their control strain (Figure 2, A, B, F).

## *Expanded Splenic Mast Cell Progenitor Population in W$^{sh}$*

Although the W$^{sh}$ mutation impairs *Kit* expression in mast cells, its effect on *Kit* expression is variable among tissues, and enhanced expression may be observed in a regionally and developmentally regulated manner.[12] Further, signaling via Kit has been implicated in the recruitment of myeloid precursors to the spleen.[28] Accordingly, splenocyte expression of Kit was studied. Unlike splenocytes from W/W$^v$ mice, where surface Kit was rare, Kit+ cells were present in elevated proportion in W$^{sh}$ mice compared to control (Figure 3A). This finding was supported by analysis of the mast cell potential of splenocytes by stimulation with SCF and interleukin-3. These conditions are optimized to grow mast cell progenitors and thus the numbers represent the number of cells potentially capable of becoming committed mast cell progenitors, which includes the early myeloid progenitors as well as those committed to the mast cell lineage.[23,25] Indeed, the density of mast cell colonies emerging from W$^{sh}$ spleen was fourfold greater than that from B6 and 20-fold greater than that from W/W$^v$ mice (Figure 3B).

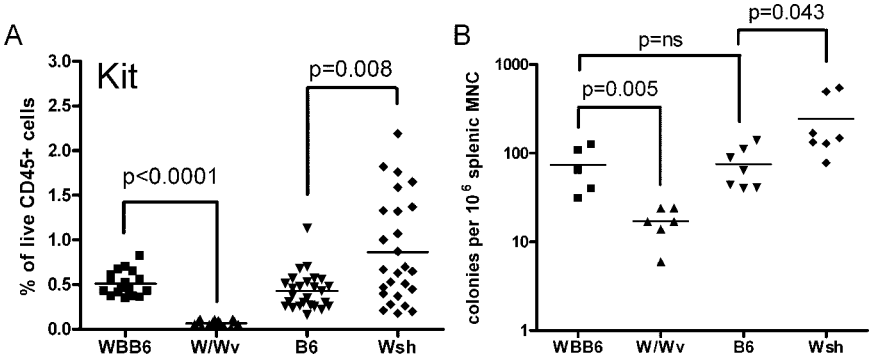


**Figure 3.** W$^{sh}$ animals exhibit an elevated proportion of cells expressing functional Kit. **A:** Surface expression of Kit in $n$ = 15 to 17 W/W$^v$ and WBB6 mice and $n$ = 22 W$^{sh}$ and B6 mice pooled from 3 to 6 independent experiments. **B:** Quantitation of splenic mast cell progenitor populations in W/W$^v$, WBB6, W$^{sh}$, and B6 mice. Note that W$^{sh}$ mice demonstrate a fourfold higher frequency per $10^6$ mononuclear cells as compared with B6 and a 20-fold excess compared to W/W$^v$ ($n$ = 5 to 7 mice per group pooled from 2 separate experiments with similar results). MNC, mononuclear cells.

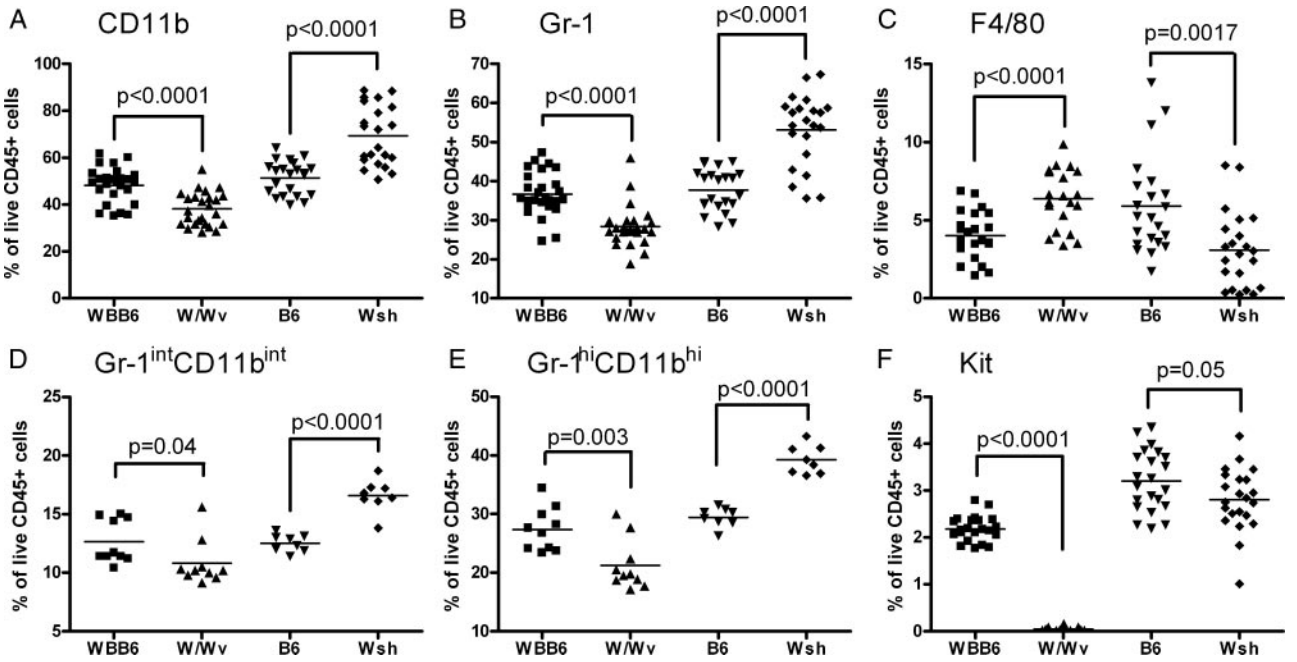


**Figure 4.** Bone marrow is neutropenic in W/W$^{v}$ and neutrophilic in W$^{sh}$ mice. Cytofluorimetric analysis of CD45+ bone marrow populations in W/Wv, WBB6, W$^{sh}$, and B6 mice ($n$ = 10 to 26 W/W$^{v}$ and WBB6 mice and $n$ = 9–22 W$^{sh}$ and B6 mice pooled from 2 to 6 independent experiments). **A:** CD11b. **B:** Gr-1. **C:** F4/80. **D:** Cells co-expressing Gr-1 and CD11b at an intermediate level. **E:** Cells co-expressing Gr-1 and CD11b at a high level. **F:** C-kit.

## *Divergent Aberrancy in Marrow and Blood in W$^{sh}$ and W/W$^{v}$*

Whether these hematological abnormalities extended to the bone marrow was then investigated. Consistent with earlier results, cells expressing CD11b and Gr-1 were expanded in W$^{sh}$ marrow and diminished in W/W$^{v}$ marrow, though F4/80 expression was inversely affected (Figure 4A–C). Both Gr-1$^{hi}$CD11b$^{hi}$ and Gr-1$^{int}$CD11b$^{int}$ populations were expanded in W$^{sh}$ mice (Figure 4, D and E). Kit expression in W$^{sh}$ was similar or slightly decreased, while it was essentially undetectable in W/W$^{v}$ individuals (Figure 4F). Again, B and T cells proportions were reciprocally reduced while CD11c expression was equivalent (data not shown).

Finally, circulating blood parameters in W$^{sh}$ and W/W$^{v}$ mice were quantified. As has been described, W/W$^{v}$ mice were anemic, while W$^{sh}$ mice displayed mean hematocrit values similar to those of B6 animals, though with a wider scatter among individuals (data not shown). Consistent with observations in the spleen and marrow, W$^{sh}$ mice exhibited an almost 70% increase in absolute circulating neutrophils compared with B6 controls (0.92 ± 0.10 vs. 0.55 ± 0.09 × $10^3$ cells/$\mu$L, $P$ = 0.008), while W/W$^{v}$ mice manifested a 40% decrease relative to WBB6 (0.32 ± 0.05 vs. 0.53 ± 0.07 × $10^3$ cells/$\mu$L, $P$ = 0.03) (Figure 5A). Finally, in keeping with the megakaryocytosis observed in spleen, and quite distinct from the other strains tested, W$^{sh}$ mice exhibited a previously undescribed thrombocytosis (1824 ± 114 vs. 1155 ± 37 × $10^3$ cells/$\mu$L, $P < 0.0001$) (Figure 5B).

Since these results differed in certain respects from those of other authors who have compared W$^{sh}$ and B6 mice aged 7 to 9 weeks,[20] a potential age-dependence of the hematopoietic phenotype was examined using 7 to 8 week-old mice (9 male animals pooled from 2 independent experiments). Indeed, splenomegaly was less pronounced in the younger animals, though still evident (W$^{sh}$ 0.086 ± 0.004g versus B6 0.069 ± 0.002g, $P$ = 0.0016). However, the relative neutrophilia in the blood and bone marrow occurred at a magnitude similar to older animals

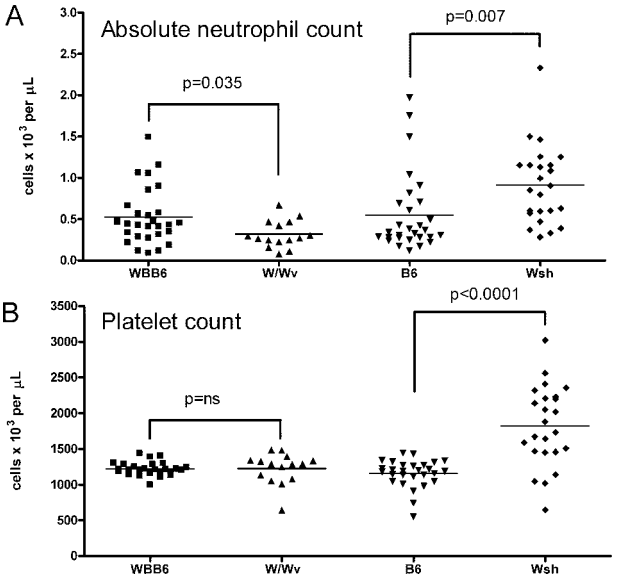


**Figure 5.** W$^{sh}$ mice exhibit circulating neutrophilia and thrombocytosis, while W/W$^{v}$ mice are mildly neutropenic. Blood from cardiac puncture was analyzed by automated cytometer to obtain complete blood count and leukocyte differential. **A:** Absolute neutrophil count. **B:** Platelet count by automated cytometer demonstrating marked elevation in W$^{sh}$ mice. Data shown represent individual mice pooled from at least 5 independent experiments ($n$ = 15 to 28 mice/group).

(bone marrow %Gr-1+ $W^{sh}$ 51.9 ± 2.5 vs. B6 39.4 ± 1.0, $P = 0.0003$; blood absolute circulating neutrophil count $W^{sh}$ 0.34 ± 0.04 × $10^3$ cells/μL versus B6 0.14 ± 0.01 × $10^3$ cells/μL, $P < 0.0001$). Similarly, splenic neutrophilia and circulating thrombocytosis were also observed at this younger age (data not shown). Accordingly, these findings suggest that younger $W^{sh}$ animals are not free of hematopoietic aberrancy.

## *Identification of the 3′ Inversion Breakpoint and Disruption of Corin in $W^{sh}$*

To understand further the genetic basis for the hematological defects observed in $W^{sh}$ mice, the causative inversion on chromosome 5 was defined. The 5′-breakpoint of the inversion had been shown to reside 2.8 to 3.3 Mb upstream of the 3′-breakpoint, somewhere between *gabrb1* and *tec*, and thereby with the potential to directly interrupt the coding sequence of 10 genes.[14] The 3′ breakpoint had been localized approximately 72 kb upstream of *Kit*, extinguishing the influence of a locus control region important for mast cell *Kit* expression.[15,16] PCR analysis with primers flanking this region amplified product from wild-type genomic DNA, but not $W^{sh}$ template (Figure 6, A and B), thus confirming these findings. Three nested reverse primers for sequencing immediately downstream of the predicted 3′ breakpoint were used to perform a "DNA walking" reaction using wild-type or $W^{sh}$ template. Sequencing of a single 500-bp product amplified from $W^{sh}$, but not wild-type, genomic DNA revealed that the entire fragment was homologous to an inverted intron of *corin*, a gene residing within the region proposed to contain the 5′ breakpoint. PCR using several pairs of primers designed to flank the predicted 3′ breakpoint amplified the expected products from $W^{sh}$ but not wild-type template (eg, Figure 6A). Sequence analysis confirmed the exact site of the 3′ breakpoint at Ensembl (release 49) position 75,903,511(+) between bases C and T, 67.5 kB upstream of the *Kit* start sequence, with an insertion of the bases TC (Figure 6B).

Based on the sequence brought to the 3′ breakpoint from *corin*, the predicted site of the 5′ breakpoint resides at Ensembl position 72,790,584(−) between bases C and G (reverse strand). This position lies between exons 5 and 6 of *corin*. Multiple attempts to amplify a PCR product using primers expected to flank the 5′ endpoint were unsuccessful, raising concerns about potential loss or addition of genetic material at that breakpoint. To delimit the extent of such anomaly, we performed genomic PCR for sequences in intron 5 and exon 6 of *corin*, immediately upstream of the inversion, and found both to be intact (Figure 6C). To evaluate for substantial loss within the inversion itself, we evaluated expression of the first potentially vulnerable gene at the newly 5′ end (*pdgfra*) and found expression of PDGF receptor on thymic stromal cells to be normal (data not shown).

Disruption of *corin* itself was confirmed by quantitative PCR analysis of transcripts encompassing exons 3 to 4, 5 to 6, and 10 to 11. These analyses revealed low levels of a truncated transcript corresponding to the inverted exons in atria of $W^{sh}$ mice; no mRNA from remaining *corin* exons was detected (Figure 6D). As a consequence, $W^{sh}$ mice exhibit cardiac hypertrophy, a phenotype characteristic of corin-deficient mice (Figure 6E).[24] These data confirm that the mutation underlying the $W^{sh}$ phenotype interrupts *corin* between exons 5 and 6, and encompasses 27 other genes in an inversion spanning approximately 3.1 Mb (Table 1). We cannot exclude the loss of a limited amount of genetic material at the newly 5′ end of

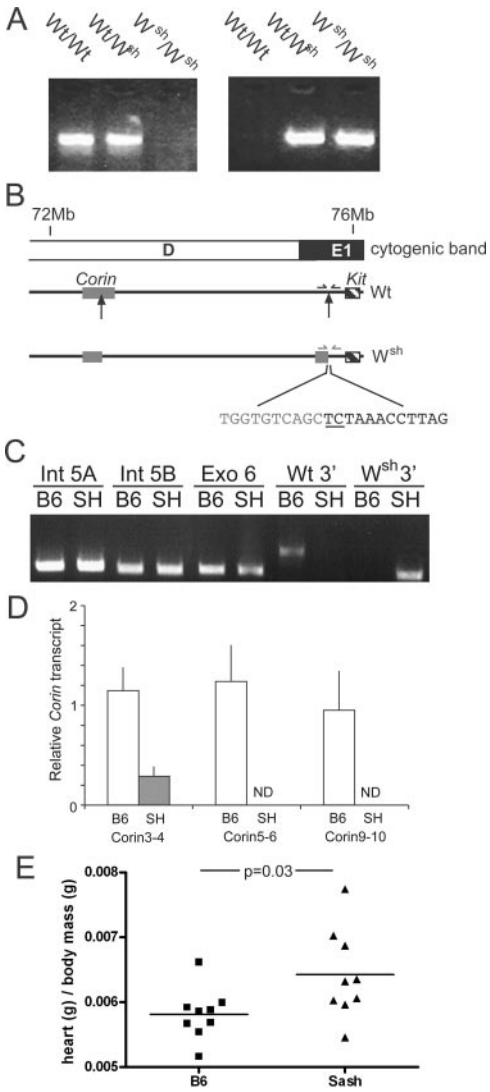


**Figure 6.** Precise definition of the $W^{sh}$ inversion mutation. **A:** Products from PCR of Wt/Wt, Wt/$W^{sh}$ and $W^{sh}$/$W^{sh}$ genomic DNA using primers flanking the sites of the 3′ breakpoint in the wild-type allele (Wt = C57BL/6J) or $W^{sh}$ allele. **B:** Schematic representation (not to scale) of $W^{sh}$ inversion on chromosome 5 showing only *corin* and *Kit* (at least 21 genes intervene). **Arrows** point to sites of 5′ and 3′ breakpoints on W and consequent inversion on $W^{sh}$. Gray nucleotides belong to inverted *corin*, underlined and italicized bases are insertions and black nucleotides are bases upstream of *Kit* unaffected by inversion. **C:** Products from genomic PCR using primers designed to *corin* regions immediately upstream of the 5′ breakpoint. Two regions of intron 5 (Int 5A and Int 5B) and most of exon 6 (Exo 6) were assayed alongside controls for the Wt and $W^{sh}$ alleles. **D:** Quantitative PCR analyses of transcripts for various *corin* exon pairs were performed using RNA prepared from wild-type ($n = 5$) or $W^{sh}$ ($n = 6$) atria. Data were normalized to a single wild-type data set and the mean and SD are shown. ND, not detected. **E:** Heart weight relative to total body weight from wild-type ($n = 9$) and $W^{sh}$ ($n = 9$) male mice aged 7 to 8 weeks pooled from 2 experiments.

**Table 1.** Genes Inverted in W$^{sh}$ (c-*kit* → *corin*)

| Gene abbreviation | Full name |
|---|---|
| *Pdgfra* | Platelet derived growth factor, alpha polypeptide |
| *Gsx2* | GS homeobox 2 |
| *Chic2* | Cysteine-rich hydrophobic domain 2 |
| *EG619945* | Unknown gene |
| *Lnx1* | Ligand of numb-protein X 1 |
| *Fip1l1* | FIP1 like 1 |
| *Scfd2* | Sec1 family domain containing 2 |
| *Rasl11b* | RAS-like, family 1, member B |
| *2700023E23Rik* | Unknown gene |
| *Usp46* | Ubiquitin specific peptidase 46 |
| *Spata18* | Spermatogenesis associated 18 |
| *Sgcb* | Sarcoglycan, beta (dystrophin-associated glycoprotein) |
| *BC0319011* | Unknown gene |
| *Dcun1d4* | Defective in cullin neddylation 1, domain containing 4 |
| *C130090K23Rik* | Unknown gene |
| *Ociad2* | OCIA domain containing 2 |
| *Ociad1* | OCIA domain containing 1 |
| *Fryl* | Furry homolog-like |
| *Slc10a4* | Solute carrier family 10 |
| *Slain2* | SLAIN motif family, member 2 |
| *Tec* | Cytoplasmic tyrosine kinase |
| *Txk* | TXK tyrosine kinase |
| *Npal1* | NIPA-like domain containing 1 |
| *Cnga1* | Cyclic nucleotide gated channel alpha 1 |
| *EG545758* | Unknown gene |
| *Zar1* | Zygote arrest 1 |
| *Nfxl1* | Nuclear transcription factor, X-box binding-like 1 |

the inversion, though any such loss cannot extend as far as *pdgfra*.

## Discussion

The absence of mast cells in several strains of mice has proven invaluable to elucidate the function of this lineage. Most of this work, including studies from our own group,[8,29] has been performed in W/W$^{v}$ animals, though increasingly the breeding and background advantages of W$^{sh}$ have rendered this mouse the experimental strain of choice for many investigators. Given the importance of Kit in hematopoiesis, it is perhaps not surprising that both W/W$^{v}$ and W$^{sh}$ mice bear abnormalities beyond the mast cell lineage. Unexpected, however, was the finding that these two strains diverge so sharply in the direction of their hematopoietic phenotypes. Specifically, W/W$^{v}$ animals are neutropenic in spleen, marrow and blood, while W$^{sh}$ animals exhibit a marked expansion of Gr-1+CD11b+ cells in spleen and marrow, as well as an elevated number of circulating neutrophils and platelets.

The impact of these contrasting myeloid and megakaryocyte abnormalities on the results of experiments performed with these mice will likely vary depending on the experimental system. In a mast cell-dependent asthma model, W/W$^{v}$ and W$^{sh}$ animals were found to be largely equivalent.[30] By contrast, while W/W$^{v}$ mice are resistant to autoantibody-induced arthritis unless engrafted with mast cells, W$^{sh}$ mice remain susceptible.[8,20,29] It is possible that in such a system the relative neutropenia of the W/W$^{v}$ could expose a requirement for the mast cell, as has been suggested.[20] Alternately, myeloid and megakaryocyte expansion in the W$^{sh}$ might compensate aberrantly for the missing mast cells. In yet other contexts, the W$^{sh}$ strain could exhibit an unexpected phenotype because of the expansion of Gr-1+CD11b+ cells in the spleen. These cells have been termed "regulatory myeloid cells" because of their observed impact in limiting anti-tumor immunity and generating skewing of immune responses in the Th2 direction in septic animals.[27,31,32] The relative importance of the Gr-1/CD11b-intermediate and -high populations has not been defined. Given these competing abnormalities in W/W$^{v}$ and W$^{sh}$ mice, drawing conclusions from either strain regarding the role of mast cells in the "normal animal" cannot be straightforward. However, correction of an abnormal phenotype in either strain by mast cell engraftment will remain strong *prima facie* evidence that mast cells have the capacity to fulfill a particular physiological role, at least under certain circumstances.

What underlies the phenotypic differences between W/W$^{v}$ and W$^{sh}$ mice? The W/W$^{v}$ genetic lesion is well defined: W is a null allele of *Kit*, while W$^{v}$ bears a point mutation in the cytoplasmic tail of the receptor, which greatly reduces its functional capacity as a kinase.[11] The result is reduced expression of a hypofunctional receptor. In contrast, the W$^{sh}$ mutation had not been fully defined. This strain was shown to bear an inversion of approximately 3Mb upstream of, but not involving, the *Kit* coding region.[12–15] Using restriction fragment analysis, the 3′ breakpoint was found to reside approximately 72kb upstream of *c-kit*, while the 5′ breakpoint was undefined, lying between *gabrb1* and *tec*. The inversion included a regulatory locus located approximately 150kb upstream of *Kit* that controls the expression of this receptor in mast cells, and elegant experimental work demonstrated that interference with this regulatory element is the probable cause for mast cell deficiency in the W$^{sh}$ mouse.[16]

The current results provide an improved understanding of the W$^{sh}$ inversion. The 3′ end of the inversion resides 67.5 kb 5′ to the coding region of *Kit* in a region devoid of known genes. The 5′ breakpoint resides between exons 5 and 6 of *corin*, disrupting that gene. While it is possible that some genetic material has been lost at the newly 5′ end of the inversion, this loss does not encompass the most proximal of the 27 inverted genes.

In addition to defining the genetic basis for the W$^{sh}$ phenotype, the precise identification of the 3′ breakpoint provides a rapid and reliable PCR genotyping assay not previously available. This assay enables breeding of the W$^{sh}$ mutation into white mice, such as BALB/c and NOD, where the characteristic coat phenotype of W$^{sh}$ heterozygotes and homozygotes would not be observed. PCR genotyping opens the door to further studies of the impact of mast cell deficiency on a variety of spontaneous diseases.

Although dysregulation of *Kit* is the likely cause of the observed hematopoietic abnormalities, the inactivation of *corin* by the 5′ breakpoint revealed here must also be considered. *Corin* encodes a cardiac transmembrane

serine protease that activates pro-atrial natriuretic peptide by cleavage.[33] Roles in the regulation of adipocytes and hair color have also been reported, and expression of the gene in kidney, testis, gravid uterus, and developing bone has been identified by Northern blot and *in situ* hybridization.[34–36] *Corin*-deficient mice exhibit mild hypertension and cardiac hypertrophy, but otherwise appear normal, although no hematological characterization has been reported.[33]

Beyond *corin* itself, it is possible that regulatory elements associated with genes in the immediate neighborhood of *corin* may have been disturbed, or that genes within the inversion may manifest altered activity. Unfortunately, little is known about potential hematopoietic functions for most of these genes. The exception is *tec*, encoding a cytoplasmic src-related kinase and strongly expressed in hematopoietic cells, including murine bone-marrow-derived mast cells and fetal liver megakaryocytes.[37,38] Interestingly, tec protein physically associates with Kit and is phosphorylated in response to SCF stimulation.[39] Tec is also phosphorylated in response to ligation of c-Mpl by thrombopoietin, and has therefore been implicated in the homeostasis of the megakaryocyte population, an association of potential relevance given the megakaryocytosis and thrombocytosis phenotype demonstrated here.[40] Beyond *tec*, the presence in the inversion of a potential X-box binding transcription factor (*Nfxl1*) is notable. It is therefore possible that defects in *corin* or other genes modify the outcome of *Kit* dysregulation in $W^{sh}$ mice to give rise to the unique phenotype observed in this strain.

A further contributor to the $W^{sh}$ phenotype is its mixed genetic background. The $W^{sh}$ mutation arose in an F1 C3H/HeH × 101/H. The commercial source for these animals reports that the animal has been backcrossed at least 10 generations to C57BL/6, leaving the thoroughness of this backcross in some uncertainty. Further, the immediate genetic environment of the $W^{sh}$ locus will remain that of the founder strain. For example, the first gene immediately upstream of the inversion, *Atp10 d* encoding a P-type ATPase, is mutated to include a premature stop codon in B6, while no such mutation is present in other strains including C3H/He.[41]

The present results contrast with prior reports of an equivalence of hematological parameters between $W^{sh}$ and B6 mice.[18,20] Although colony conditions might explain a certain degree of divergence among mice, results from these smaller studies fall within the ranges observed in the current analysis, which was numerically powered to detect interstrain differences. Thus, there exists no meaningful conflict between these data and those published previously.

In conclusion, $W/W^{v}$ and $W^{sh}$ mice exhibit abnormalities affecting hematopoietic lineages beyond the mast cell. The $W/W^{v}$ strain exhibits anemia and mild neutropenia, while the $W^{sh}$ manifests neutrophilia, thrombocytosis, splenomegaly and cardiomegaly. The genetic basis for these differences remains uncertain, but in $W^{sh}$ mice may involve defects beyond the regulation of *Kit*, given the size and complexity of the genetic inversion, including disruption of *corin*. The importance of these phenotypic differences is likely to vary with experimental context. Consideration of this aberrancy is warranted when using these important murine strains for functional study of the participation of mast cells in experimental models of disease.

## References

1. McNeil HP, Adachi R, Stevens RL: Mast cell-restricted tryptases: structure and function in inflammation and pathogen defense. J Biol Chem 2007, 282:20785–20789
2. Echtenacher B, Mannel DN, Hultner L: Critical protective role of mast cells in a model of acute septic peritonitis. Nature 1996, 381:75–77
3. Malaviya R, Ikeda T, Ross E, Abraham SN: Mast cell modulation of neutrophil influx and bacterial clearance at sites of infection through TNF-alpha. Nature 1996, 381:77–80
4. Gurish MF, Bryce PJ, Tao H, Kisselgof AB, Thornton EM, Miller HR, Friend DS, Oettgen HC: IgE enhances parasite clearance and regulates mast cell responses in mice infected with Trichinella spiralis. J Immunol 2004, 172:1139–1145
5. Thakurdas SM, Melicoff E, Sansores-Garcia L, Moreira DC, Petrova Y, Stevens RL, Adachi R: The mast cell-restricted tryptase mMCP-6 has a critical immunoprotective role in bacterial infections. J Biol Chem 2007, 282:20809–20815
6. Shin K, Watts GF, Oettgen HC, Friend DS, Pemberton AD, Gurish MF, Lee DM: Mouse mast cell tryptase mMCP-6 is a critical link between adaptive and innate immunity in the chronic phase of trichinella spiralis infection. J Immunol 2008, 180:4885–4891
7. Martin TR, Galli SJ, Katona IM, Drazen JM: Role of mast cells in anaphylaxis. Evidence for the importance of mast cells in the cardiopulmonary alterations and death induced by anti-IgE in mice, J Clin Invest 1989, 83:1375–1383
8. Nigrovic PA, Binstadt BA, Monach PA, Johnsen A, Gurish M, Iwakura Y, Benoist C, Mathis D, Lee DM: Mast cells contribute to initiation of autoantibody-mediated arthritis via IL-1, Proc Natl Acad Sci USA 2007, 104:2325–2330
9. Metz M, Grimbaldeston MA, Nakae S, Piliponsky AM, Tsai M, Galli SJ: Mast cells in the promotion and limitation of chronic inflammation. Immunol Rev 2007, 217:304–328
10. Zsebo KM, Williams DA, Geissler EN, Broudy VC, Martin FH, Atkins HL, Hsu RY, Birkett NC, Okino KH, Murdock DC, Frederick W: Jacobsen. Keith E Langley, Kent A Smith, Takashi Takeish, Bruce M Cattanach, Stephen J Galli, Sidney V Suggs: Stem cell factor is encoded at the Sl locus of the mouse and is the ligand for the c-kit tyrosine kinase receptor, Cell 1990, 63:213–224
11. Nocka K, Tan JC, Chiu E, Chu TY, Ray P, Traktman P, Besmer P: Molecular bases of dominant negative and loss of function mutations at the murine c-kit/white spotting locus: w37. Wv, W41 and W. EMBO J 1990, 9:1805–1813
12. Duttlinger R, Manova K, Chu TY, Gyssler C, Zelenetz AD, Bachvarova RF, Besmer P: W-sash affects positive and negative elements controlling c-kit expression: ectopic c-kit expression at sites of kit-ligand expression affects melanogenesis. Development 1993, 118:705–717
13. Duttlinger R, Manova K, Berrozpe G, Chu TY, DeLeon V, Timokhina I, Chaganti RS, Zelenetz AD, Bachvarova RF, Besmer P: The Wsh and Ph mutations affect the c-kit expression profile: c-kit misexpression in embryogenesis impairs melanogenesis in Wsh and Ph mutant mice. Proc Natl Acad Sci USA 1995, 92:3754–3758
14. Nagle DL, Kozak CA, Mano H, Chapman VM, Bucan M: Physical mapping of the Tec and Gabrb1 loci reveals that the Wsh mutation on mouse chromosome 5 is associated with an inversion. Hum Mol Genet 1995, 4:2073–2079
15. Berrozpe G, Timokhina I, Yukl S, Tajima Y, Ono M, Zelenetz AD, Besmer P: The W(sh), W(57), and Ph Kit expression mutations define tissue-specific control elements located between -23 and -154 kb upstream of Kit. Blood 1999, 94:2658–2666
16. Berrozpe G, Agosti V, Tucker C, Blanpain C, Manova K, Besmer P: A distant upstream locus control region is critical for expression of the Kit receptor gene in mast cells. Mol Cell Biol 2006, 26:5850–5860
17. Nakano T, Sonoda T, Hayashi C, Yamatodani A, Kanayama Y, Yamamura T, Asai H, Yonezawa T, Kitamura Y, Galli SJ: Fate of bone

marrow-derived cultured mast cells after intracutaneous, intraperitoneal, and intravenous transfer into genetically mast cell-deficient W/Wv mice. Evidence that cultured mast cells can give rise to both connective tissue type and mucosal mast cells. J Exp Med 1985, 162:1025–1043
18. Grimbaldeston MA, Chen CC, Piliponsky AM, Tsai M, Tam SY, Galli SJ: Mast cell-deficient W-sash c-kit mutant Kit W-sh/W-sh mice as a model for investigating mast cell biology in vivo. Am J Pathol 2005, 167:835–848
19. Chervenick PA, Boggs DR: Decreased neutrophils and megakaryocytes in anemic mice of genotype W/W. J Cell Physiol 1969, 73:25–30
20. Zhou JS, Xing W, Friend DS, Austen KF, Katz HR: Mast cell deficiency in Kit(W-sh) mice does not impair antibody-mediated arthritis. J Exp Med 2007, 204:2797–2802
21. Lyon MF, Glenister PH: A new allele sash (Wsh) at the W-locus and a spontaneous recessive lethal in mice. Genet Res 1982, 39:315–322
22. Wolters PJ, Mallen-St Clair J, Lewis CC, Villalta SA, Baluk P, Erle DJ, Caughey GH: Tissue-selective mast cell reconstitution and differential lung gene expression in mast cell-deficient Kit(W-sh)/Kit(W-sh) sash mice. Clin Exp Allergy 2005, 35:82–88
23. Gurish MF, Tao H, Abonia JP, Arya A, Friend DS, Parker CM, Austen KF: Intestinal mast cell progenitors require CD49dbeta7 (alpha4beta7 integrin) for tissue-specific homing. J Exp Med 2001, 194:1243–1252
24. Hallgren J, Jones TG, Abonia JP, Xing W, Humbles A, Austen KF, Gurish MF: Pulmonary CXCR2 regulates VCAM-1 and antigen-induced recruitment of mast cell progenitors. Proc Natl Acad Sci USA 2007, 104:20478–20483
25. Arinobu Y, Iwasaki H, Gurish MF, Mizuno S, Shigematsu H, Ozawa H, Tenen DG, Austen KF, Akashi K: Developmental checkpoints of the basophil/mast cell lineages in adult murine hematopoiesis. Proc Natl Acad Sci USA 2005, 102:18105–18110
26. Livak KJ, Schmittgen TD: Analysis of relative gene expression data using real-time quantitative PCR and the 2(-Delta Delta C(T)) Method. Methods 2001, 25:402–408
27. Delano MJ, Scumpia PO, Weinstein JS, Coco D, Nagaraj S, Kelly-Scumpia KM, O'Malley KA, Wynn JL, Antonenko S, Al-Quran SZ, Swan R, Chung CS, Atkinson MA, Ramphal R, Gabrilovich DI, Reeves WH, Ayala A, Phillips J, Laface D, Heyworth PG, Clare-Salzler M, Moldawer LL: MyD88-dependent expansion of an immature GR-1(+)CD11b(+) population induces T cell suppression and Th2 polarization in sepsis. J Exp Med 2007, 204:1463–1474
28. Broudy VC, Lin NL, Priestley GV, Nocka K, Wolf NS: Interaction of stem cell factor and its receptor c-kit mediates lodgment and acute expansion of hematopoietic cells in the murine spleen. Blood 1996, 88:75–81
29. Lee DM, Friend DS, Gurish MF, Benoist C, Mathis D, Brenner MB: Mast cells: a cellular link between autoantibodies and inflammatory arthritis. Science 2002, 297:1689–1692
30. Yu M, Tsai M, Tam SY, Jones C, Zehnder J, Galli SJ: Mast cells can promote the development of multiple features of chronic asthma in mice. J Clin Invest 2006, 116:1633–1641
31. Gabrilovich DI, Velders MP, Sotomayor EM, Kast WM: Mechanism of immune dysfunction in cancer mediated by immature Gr-1+ myeloid cells. J Immunol 2001, 166:5398–5406
32. Makarenkova VP, Bansal V, Matta BM, Perez LA, Ochoa JB: CD11b+/Gr-1+ myeloid suppressor cells cause T cell dysfunction after traumatic stress. J Immunol 2006, 176:2085–2094
33. Chan JC, Knudson O, Wu F, Morser J, Dole WP, Wu Q: Hypertension in mice lacking the proatrial natriuretic peptide convertase corin. Proc Natl Acad Sci USA 2005, 102:785–790
34. Garruti G, Giusti V, Nussberger J, Darimont C, Verdumo C, Amstutz C, Puglisi F, Giorgino F, Giorgino R, Cotecchia S: Expression and secretion of the atrial natriuretic peptide in human adipose tissue and preadipocytes. Obesity (Silver Spring) 2007, 15:2181–2189
35. Enshell-Seijffers D, Lindon C, Morgan BA: The serine protease Corin is a novel modifier of the Agouti pathway. Development 2008, 135:217–225
36. Yan W, Sheng N, Seto M, Morser J, Wu Q: Corin, a mosaic transmembrane serine protease encoded by a novel cDNA from human heart. J Biol Chem 1999, 274:14926–14935
37. Mano H, Mano K, Tang B, Koehler M, Yi T, Gilbert DJ, Jenkins NA, Copeland NG, Ihle JN: Expression of a novel form of Tec kinase in hematopoietic cells and mapping of the gene to chromosome 5 near Kit. Oncogene 1993, 8:417–424
38. Kluppel M, Donoviel DB, Brunkow ME, Motro B, Bernstein A: Embryonic and adult expression patterns of the Tec tyrosine kinase gene suggest a role in megakaryocytopoiesis, blood vessel development, and melanogenesis. Cell Growth Differ 1997, 8:1249–1256
39. Tang B, Mano H, Yi T, Ihle JN: Tec kinase associates with c-kit and is tyrosine phosphorylated and activated following stem cell factor binding. Mol Cell Biol 1994, 14:8432–8437
40. Yamashita Y, Miyazato A, Shimizu R, Komatsu N, Miura Y, Ozawa K, Mano H: Tec protein-tyrosine kinase is involved in the thrombopoietin/c-Mpl signaling pathway. Exp Hematol 1997, 25:211–216
41. Flamant S, Pescher P, Lemercier B, Clement-Ziza M, Kepes F, Fellous M, Milon G, Marchal G, Besmond C: Characterization of a putative type IV aminophospholipid transporter P-type ATPase. Mamm Genome 2003, 14:21–30